



HAL
open science

Role of driving scales in a model of coronal heating

O. Podladchikova, B. Lefebvre, Vladimir Krasnoselskikh

► **To cite this version:**

O. Podladchikova, B. Lefebvre, Vladimir Krasnoselskikh. Role of driving scales in a model of coronal heating. SOLAR WIND TEN: Proceedings of the Tenth International Solar Wind Conference, 2003, Pisa, Italy. pp.311-314, 10.1063/1.1618601 . insu-02926769

HAL Id: insu-02926769

<https://insu.hal.science/insu-02926769>

Submitted on 1 Sep 2020

HAL is a multi-disciplinary open access archive for the deposit and dissemination of scientific research documents, whether they are published or not. The documents may come from teaching and research institutions in France or abroad, or from public or private research centers.

L'archive ouverte pluridisciplinaire **HAL**, est destinée au dépôt et à la diffusion de documents scientifiques de niveau recherche, publiés ou non, émanant des établissements d'enseignement et de recherche français ou étrangers, des laboratoires publics ou privés.

Role of driving scales in a model of coronal heating

O. Podladchikova^{*†}, B. Lefebvre^{*} and V. Krasnoselskikh^{*}

**LPCE/CNRS & Université d'Orléans UMR 6115
3A av. de la Recherche Scientifique, 45071 Orléans, FRANCE
†Kiev Polytechnic Institute, Kiev, UKRAINE*

Abstract. Models of coronal heating based on the dissipation of small-scale current sheets generally assume energy injection at large scales by photospheric motions. However due to the nature of these motions, excitation mechanisms may occur on a wide range of scales. We study the role of the dominant scales of energy injection in the framework of the lattice model introduced in [1]. In particular it is shown that as the weight of large scales increases, the probability densities of dissipated energy and of waiting times between heating events develops fatter tails tending toward power-laws.

INTRODUCTION

The dissipation of many small scale current sheets resulting in the so-called nano-flares was conjectured by Parker to be a mechanism of coronal heating [2]. Various formation mechanisms of these small scale currents have been proposed, whose origin ultimately lies in photospheric convection inducing complex motions of coronal magnetic field lines footpoints.

Observed statistics of flare, microflares, and smaller events have suggested a certain scale-invariance between these phenomena ([3, 4] and references therein). Extrapolation of a power-law distribution for the dissipated energy to smaller energies indicate that heating by nanoflares is a viable mechanism if its index is smaller than -2 [5]. Different interpretations of recent observations in EUV of small scale events in terms of dissipated energy provide indices scattered around -2 [6, 7, 8] thereby leaving the question quite open.

These particular statistics have stimulated a number of simple (lattice) models whose statistics can be extensively studied. For instance, flare models based on Self-Organized-Criticality (SOC) [9, 10] have met some success in reproducing certain statistics of observed flare and micro-flare associated emissions [4]. Especially for applications to coronal heating, it is essential to provide lattice models allowing for a clear interpretation by physical processes rather than concentrating on SOC (e.g. [11, 12, 13, 1, 14]). The model we shall consider here is the one introduced in [1] whose two fundamental elements are on one hand the dissipative processes mimicking anomalous resistivity or magnetic reconnection and on the other hand the sources perturbing the magnetic field configuration and generating the currents.

The emphasis in this note shall be on the role played by the dominant scales in the source term of the model. Either Parker's model or models of coronal heating based on MHD turbulence explicitly make the classical assumption that energy is injected at large scales only from photospheric motions and cascades down to small scales [15]. However, photospheric convection involves a wide range of different motions, including shear-generated turbulent-like fluctuations between granules [16]. Sources perturbing the system on a wide range of scales are likely to affect its dynamics, having some effects on the energy dissipation and conversion into heat. This is what we are going to study in the framework of the lattice model of [1] using sources with a power-law spectrum. This form easily allows to change the relative weights of the different characteristic scales of the source term.

MODEL

The model consists of magnetic field distributed into cells of a 2D grid, perpendicular to the grid, and subject to driving and dissipation mechanisms. Such a simplification allows to easily select between different sources and dissipation mechanisms. Periodic boundary conditions on a square grid of size $N \times N$ are assumed.

The source spectrum is a power-law spectrum in a certain range of wavenumbers. This allows to easily control the relative weights of different wavenumbers, thereby controlling the dominant scales of energy injection. Therefore the source provides a magnetic field in-

crement of the form

$$\delta B(x, y, t) = C_{\alpha, k_{\min}, k_{\max}} \sum_{k_x, k_y} |\mathbf{k}|^{-\alpha} e^{i(k_x x + k_y y + \phi(t))}, \quad (1)$$

where C is such that the total intensity is normalized to 1. The phases ϕ are independent random variables uniformly distributed in $[0, 2\pi)$. The dominant scales in δB can be controlled by changing both α and the range of wavenumbers in the summation.

The dissipation mechanisms considered in our previous studies are of two types, namely reconnection or anomalous resistivity. Both depend on currents, which propagate on the border of the cells and are computed as $\mathbf{j} = \nabla \times \mathbf{B}$. Anomalous resistivity arises when a current exceeds a given threshold as the result of micro-instabilities. Reconnection in this simple framework requires an additional condition mimicking an X-point. In both cases, the energy dissipated into heat is supposed to be proportional to j^2 . See [1] for more details. In the following the grid size is 256×256 , dissipation is provided by anomalous resistivity, and the dissipation threshold is $j_{\max} = 3$.

MULTISCALE DRIVING

In this section the source acts at all available scales, but different exponents in eq. (1) are used. In particular, the case $\alpha = 0$ corresponds to white (in space) noise [1, 17].

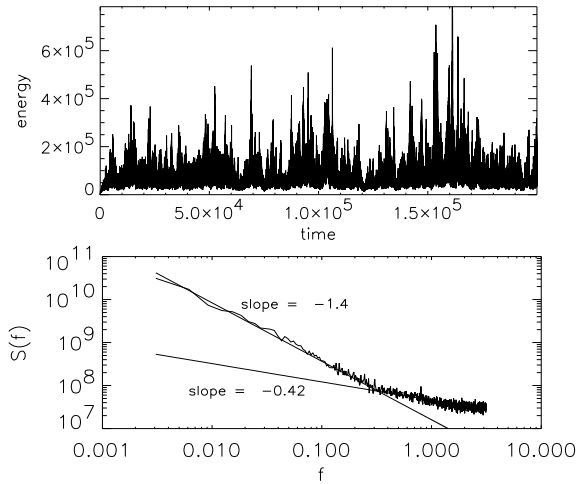


FIGURE 1. Time series of the total dissipated energy over the grid and its power spectrum for $\alpha = -2$.

As α increases, the time series of the total dissipated energy displays more intense and sporadic bursts (Fig. 1). At the same time, the power-spectrum tends toward a more pronounced power-law shape (Fig. 1, lower panel). This power-law breaks down at high-frequencies, where the spectrum flattens. This breaking point drifts toward

higher-frequencies as α increases. Interestingly on each side of the breaking point spectra weakly depend on α , at least in the interval $[1, 3]$.

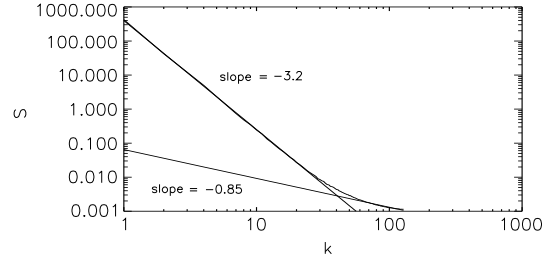


FIGURE 2. Power spectrum in k of the magnetic field for $\alpha = -2$.

The spatial power spectrum of B shows a similar tendency to a power-law at small k which breaks down to a flatter spectrum at small scales (Fig. 2). The energy contained in the steepest part and at the largest scales increases relatively to the energy contained in the small scale part when α increases (96% for $\alpha = 1$, 99% for $\alpha = 1$ and 99.8% for $\alpha = 3$). At large scales the spectrum decreases faster than the source, which means that the development of the “cascade” is somehow slowed down.

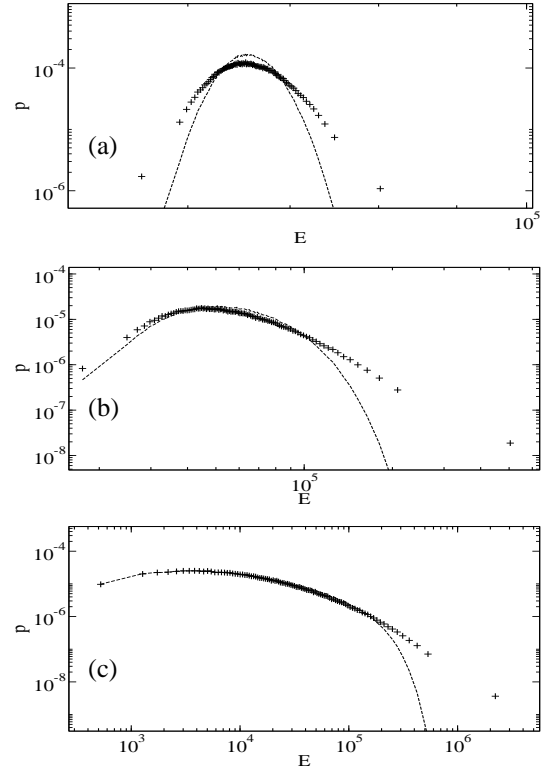


FIGURE 3. Log-log plot of the dissipated energy PDF for different values of α . (a) $\alpha = 1$, (b) $\alpha = 2$, (c) $\alpha = 3$. The dashed line represents the Gaussian with same mean and variance.

White noise sources combined with anomalous resistivity dissipation provide dissipated energies whose Probability Density Functions (PDF) weakly depart from the Gaussian [1]. When α increases to positive values, this departure is more and more marked by a heavy tail corresponding to large deviations toward high energy events (Fig. 3). However the tail does not tend toward a power-law, since on the log-log plot it exhibits clear concavity. A more precise characterization could be provided using Pearson curves [18]. Another statistics of solar flares extensively discussed is the waiting time distribution between two solar flares (here between two peaks of dissipated energy above a given threshold). For $\alpha = 3$ it follows a power-law (Fig. 4), in agreement with some observations (see the discussion concluding the paper).

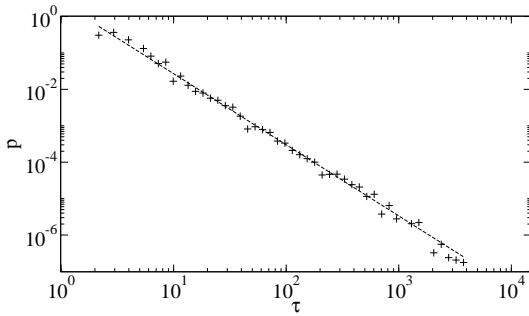


FIGURE 4. PDF of waiting times for $\alpha = -3$. A least-squares power-law fit (dashed line) yields an exponent -1.95 ± 0.10 .

The source also has an effect on the spatial characteristics of the magnetic field. In [17] these characteristics were studied by Singular Value Decomposition (SVD). From the singular values μ_k it is possible to obtain an entropy which provides a quantitative estimate of spatial complexity, defined as [19, 17]

$$H = - \lim_{N \rightarrow \infty} \frac{1}{\ln N} \sum_{k=1}^N E_k \ln E_k,$$

with $E_k = \mu_k^2 / \sum_i \mu_i^2$. H is defined in such a way that $H = 1$ when energy is equidistributed over all singular modes (maximal disorder) and $H = 0$ when all the variance is contained in a single mode (minimal disorder).

TABLE 1. Entropy as a function of the exponent α defined in eq. (1).

α	0	1	2	3
H	0.75	0.55	0.22	0.12

As clearly seen in Table 1, the entropy significantly decreases when α increases. Thus when large scales are given more and more weight in the sources, the magnetic field has a natural tendency to have a more coherent structure at large scales.

DRIVING AT LARGE SCALES

Here we consider a quasi-periodic source involving only the two largest modes.

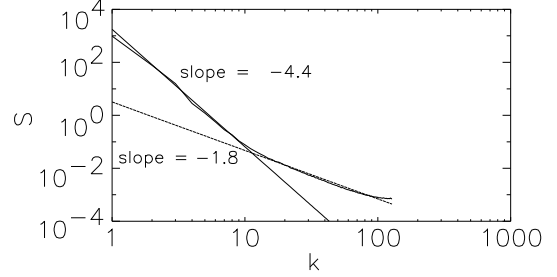


FIGURE 5. Power spectrum in k of the magnetic field, when the system is driven by the two largest modes.

Although the system is driven only at large scales, the spectrum develops toward smaller scales due to the local coupling between cells. In a statistically steady state, it may be approximated by a power-law which flattens at small scales (Fig. 5). The dissipated energy PDF displays a fat high-energy tail which can be roughly approximated by a power-law, with rather small exponent -1.19 ± 0.08 . The waiting time distribution also exhibits a slowly decaying tail (Fig. 7), with a power-law shape with exponent -2.28 ± 0.12 .

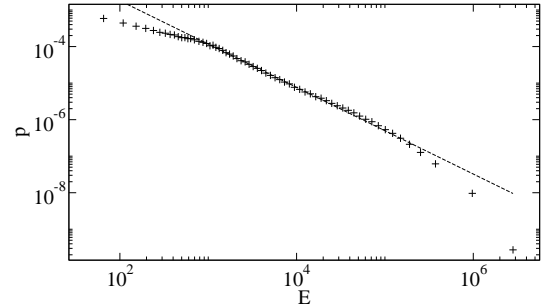


FIGURE 6. PDF of the dissipated energy. A power-law fit to its tail (dashed line) has exponent -1.19 ± 0.08 .

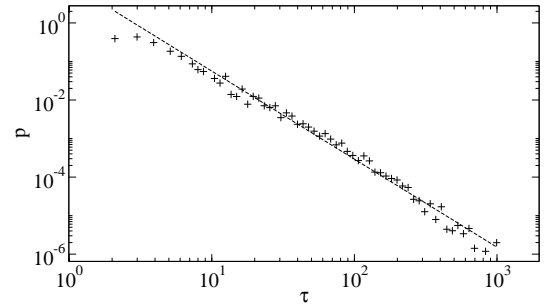


FIGURE 7. PDF of waiting times. A power-law fit to its tail (dashed line) has exponent -2.28 ± 0.12 .

DISCUSSION

The role of the scales in the source term of a lattice model for coronal heating was studied. For this purpose a power-law spectrum was used, increasing the relative role of large scales with respect to the limit case of white-noise-in-space sources considered in [1, 17].

The magnetic field fluctuations appear to have a power-law spectrum which is at large scales generally steeper than the one of the source, showing that the system does not exhibit a trivial response to the source but rather is ruled by its own dynamics. Particularly at small scales it is rather insensitive to the form of the source's spectrum. Furthermore, a similar power-law power spectrum appears when the system is driven only at large scales, showing that it is an intrinsic feature of such a model when large scales dominate the energy injection.

As the weight of large scales plays a more significant role in energy injection, a long tail is formed in the PDF of dissipated energy as well as in the waiting time distribution between energetic events. Indeed, in this case large scale gradients form and their dissipation produces rare but energetic dissipative events resulting from many small-scale local dissipations.

The power-laws found in the PDF of dissipated energy are in poor agreement with those found in experiment: the exponents are too small or the tail does not convincingly follow a power-law, and the PDF steepens toward high energies although flares seem to follow a flatter distribution than microflares and nanoflares. This situation may improve by considering sources with potentially large amplitude as found in [20], or using a different and more sophisticated dissipation process such as the reconnection used in [1, 17] and which was shown to produce significant changes in the statistics of dissipated energy and fatter tails in its PDF.

However, we have found heavy tails in waiting time distributions, whose power-law decay seems to agree with most observations [21, 22, 23]. Attention on waiting time distribution was drawn in particular by the remark that pure SOC models exhibit only a Poisson waiting time distribution [22]. Attempts to correct this have used “non-conventional” properties of the source, whereas they are non-stationary [24] or correlated [25] in time, or acting continuously in time [26]. The present study suggests that sources acting at large scales or representing a wideband spectrum dominated by large scales (as can be expected on physical grounds) also help to recover a more correct waiting time distribution.

ACKNOWLEDGMENTS

The authors are thankful the Referee for his help to improve the presentation of this paper. BL acknowledges financial support from the CNES.

REFERENCES

1. Krasnoselskikh, V., Podladchikova, O., Lefebvre, B., and Vilmer, N., *A&A*, **382**, 699–712 (2002).
2. Parker, E. N., *ApJ*, **330**, 474–479 (1988).
3. Aschwanden, M. J., Poland, A., and Rabin, D., *Annu. Rev. Astron. Astrophys.*, **39**, 175–210 (2001).
4. Georgoulis, M. K., Vilmer, N., and Crosby, N. B., *A&A*, **367**, 326–338 (2001).
5. Hudson, H. S., *Solar Physics*, **133**, 357–369 (1991).
6. Benz, A., and Krucker, S., *Sol. Phys.*, **182**, 349–363 (1998).
7. Mitra-Kraev, U., and Benz, A. O., *A&A*, **373**, 318–328 (2001).
8. Aschwanden, M. J., Tarbell, T. D., Nightingale, R. W., Schrijver, C. J., Title, A., Kankelborg, C. C., Martens, P., and Warren, H. P., *ApJ*, **535**, 1047–1065 (2000).
9. Lu, E. T., and Hamilton, R. J., *ApJ*, **380**, L89–L92 (1991).
10. Charbonneau, P., McIntosh, S., Han-Li, L., and Bogdan, T., *Solar Phys.*, **203**, 321 (2001).
11. Isliker, H., Anastasiadis, A., Vassiliadis, D., and Vlahos, L., *A&A*, **335**, 1085–1092 (1998).
12. Einaudi, G., and Velli, M., *Phys. Plasmas*, **6**, 4146–4153 (1999).
13. Longcope, D. W., and Noonan, E. J., *ApJ*, **542**, 1088–1099 (2000).
14. Buchlin, E., Aletti, V., Galtier, S., Velli, M., and Vial, J., *these proceedings* (2002).
15. Gómez, D. O., Dmitruk, P. A., and Milano, L. J., *Solar Phys.*, **195**, 299–318 (2000).
16. Nesis, A., Hammer, R., Kiefer, M., Schleicher, H., Sigwarth, M., and Staiger, J., *A&A*, **345**, 265–275 (1999).
17. Podladchikova, O., Dudok de Wit, T., Krasnoselskikh, V., and Lefebvre, B., *A&A*, **382**, 713–721 (2002).
18. Podladchikova, O., PhD thesis, Université d’Orléans, 2002.
19. Aubry, N., Guyonnet, R., and Lima, R., *J. Stat. Phys.*, **64**, 683–739 (1991).
20. Georgoulis, M., and Vlahos, L., *ApJ*, **469**, L135 (1996).
21. Wheatland, M. S., Sturrock, P. A., and McTiernan, J. M., *ApJ*, **509**, 448–455 (1998).
22. Boffetta, G., Carbone, V., Giuliani, P., Veltri, P., and Vulpiani, A., *Phys. Rev. Lett.*, **83**, 4662–4665 (1999).
23. Lepreti, F., Carbone, V., and Veltri, P., *ApJ*, **555**, L133–L136 (2001).
24. Norman, J. P., Charbonneau, P., McIntosh, S. W., and Liu, H., *ApJ*, **557**, 891–896 (2001).
25. Sanchez, R., Newman, D., and Carreras, B., *Phys. Rev. Lett.*, **88**, 068302 (2002).
26. Hamon, D., Nicodemi, M., and Jensen, H., *A&A*, **387**, 326–334 (2002).